

# Transition metal complexes (M = Cu, Ni and Mn) of Schiff-base ligands: Syntheses, crystal structures, and inhibitory bioactivities against urease and xanthine oxidase

Yu-Guang Li <sup>a</sup>, Da-Hua Shi <sup>a</sup>, Hai-Liang Zhu <sup>a,\*</sup>, Hong Yan <sup>a</sup>, Seik Weng Ng <sup>b</sup>

<sup>a</sup> School of Life Sciences & School of Chemistry and Chemical Engineering, Nanjing University, Nanjing 210093, PR China

<sup>b</sup> Department of Chemistry, University of Malaya, 50603 Kuala Lumpur, Malaysia

Received 24 August 2006; received in revised form 31 January 2007; accepted 1 February 2007

Available online 20 February 2007

## Abstract

Six new transition metal complexes (M = Cu(II), Ni(II) and Mn(III)) of tridentate (H<sub>2</sub>L<sup>1</sup>, HL<sup>2</sup>) and/or bidentate (HL<sup>3</sup>, HL<sup>4</sup>) Schiff-base ligands, obtained from the condensation of salicylaldehyde with glycine, *N*-(2-aminoethyl)morpholine, 4-(2-aminoethyl)phenylic acid and 4-(2-aminoethyl)benzulfamide, respectively, were synthesized and structurally determined by single-crystal X-ray analysis. Complexes **1–6** were evaluated for their effect on the *jack bean* urease and xanthine oxidase (XO). Copper(II) complexes **1–3** (IC<sub>50</sub> = 0.43–2.25 μM) showed potent inhibitory activity against *jack bean* urease, comparable with acetohydroxamic acid (IC<sub>50</sub> = 42.12 μM), which is a positive reference. And these copper(II) complexes (IC<sub>50</sub> = 10.26–15.82 μM) also exhibited strong ability to inhibit activity of XO, comparable to allopurinol (IC<sub>50</sub> = 10.37 μM), which was used as a positive reference. Nickel(II) and manganese(III) complexes **4–6** showed weak inhibitory activity to *jack bean* urease (IC<sub>50</sub> = 4.36–8.25 μM) and no ability to inhibit XO (IC<sub>50</sub> > 100 μM).

© 2007 Elsevier B.V. All rights reserved.

**Keywords:** Complexes; Schiff bases; Crystal structures; Urease inhibitors; Xanthine oxidase inhibitors

## 1. Introduction

In the past decades, the complexes containing transition metal ions and various Schiff-base ligands have been extensively investigated due to their novel structures and potential applications in many fields [1]. Particularly, a large number of transition metal complexes of Schiff-base ligands derived from the condensation of salicylaldehyde and its derivatives with various primary amines become the hot topics of contemporary research [2]. These Schiff-base ligands may act as a bidentate N,O- [3] and a tridentate N,O,O-donor ligand [4], and so on, which can be designed to yield mono-, bi-, dimer,

1D, 2D, 3D complexes [5] together with other coordinating moieties such as azide ion, thiocyanate and carboxylic group acting as either a bridging or a terminal ligand. The use foreground of such metal complexes is also promising such as acting as single-molecule magnets (SMMs) [6], as luminescent probes [7], as catalysts for specific DNA [8,9] and RNA [10] cleavage reactions. In order to have an insight into the potential application of complexes of Schiff-base ligands as an enzyme inhibitor against urease and xanthine oxidase (XO), we have designed and synthesized six new complexes of Cu, Ni, Mn containing Schiff-base ligands derived from the condensation of salicylaldehyde and various primary amines.

Urease, the first enzyme crystallized to be shown to possess nickel ions [11], is an important enzyme in both agriculture and medicine, which rapidly catalyzes the

\* Corresponding author. Tel.: +0086 25 8359 2572; fax: +0086 25 8359 2672.

E-mail address: [zhuhl@nju.edu.cn](mailto:zhuhl@nju.edu.cn) (H.-L. Zhu).

hydrolysis of urea to form ammonia and carbamic acid [12]. But the end byproduct of such decomposing reactions also results in a pH increase, responsible for negative effects of urease activity in human health [13], such as causing peptic ulcers, stomach cancer, etc., and agriculture, for example, the efficiency of soil nitrogen fertilization with urea decreases due to ammonia volatilization and root damage caused by soil pH increase [14]. It's interesting to control the activity of urease through the use of inhibitors in order to counteract these negative effects. Some matters possessing inhibitory activity against urease have been reported such as boric acid [15], fluoride [16], heavy metal ions [17],  $\alpha$ -hydroxyketones [18].

However, XO catalyzes the hydroxylation of hypoxanthine and of xanthine to yield uric acid and superoxide anions. The latter has been linked to post ischaemic tissue injury and edema as well as to vascular permeability [19]. XO may reduce pharmacological properties of synthetic purine drugs, such as antileukaemic 6-mercaptopurine, through oxidization reaction [20]. Controlling the activities of XO may be helpful to the therapy of some correlative diseases. Nowadays, as a potent inhibitor of XO allopurinol to treat gout has been known for a long time [21]. But reports on inhibitory activity against the XO of Schiff-base complexes are very rare in the literature [22].

In this paper, we reported the synthesis of six d-transition metal complexes **1–6** ( $M = \text{Cu, Ni, Mn}$ ) and investigated their inhibitory activities against urease and XO. The crystal structures of these complexes with Schiff-base ligands  $L^{1-4}$  derived from the condensation of salicylaldehyde with glycine, *N*-(2-aminoethyl)morpholine, 4-(2-amino-ethyl)phenylic acid, and 4-(2-aminoethyl)benzulfamide, respectively, were determined by X-ray analysis: Complex  $[(\text{CuL}^1)_2 \cdot 1/3(\text{CH}_3\text{OH})]_n$  (**1**);  $[\text{CuL}^2(\text{Py})(\text{H}_2\text{O})](\text{ClO}_4) \cdot \text{H}_2\text{O}$  (**2**);  $[\text{Cu}(\text{L}^3)_2] \cdot 2\text{H}_2\text{O}$  (**3**);  $[\text{Ni}(\text{L}^3)_2] \cdot 2\text{H}_2\text{O}$  (**4**);  $[\text{Ni}(\text{L}^4)_2]$  (**5**);  $[\text{Mn}_2(\text{L}^4)_2(\text{N}_3)_2] \cdot 2\text{CH}_3\text{OH}$  (**6**).

## 2. Experimental

### 2.1. Materials and physical measurements

All the chemicals used in syntheses were of reagent grade and were used without further purification.  $\text{HL}^3$  and  $\text{HL}^4$  ligands were obtained as described in the literature [23,24].

Elemental analyses for C, H and N were carried out on a Perkin–Elmer 2400 analyzer. IR spectra were recorded using KBr pellets ( $4000\text{--}400\text{ cm}^{-1}$ ) on a Nexus 870 FT-IR spectrophotometer. Electronic spectra in the 200–800 nm range were measured using DMSO– $\text{H}_2\text{O}$  (1:1 v/v) solution on a Shimadzu UV-160 A spectrophotometer.

### 2.2. Synthesis

#### 2.2.1. Synthesis of $[(\text{CuL}^1)_2 \cdot 1/3(\text{CH}_3\text{OH})]_n$ (**1**)

Salicylaldehyde (0.24 g, 2.0 mmol) and glycine (0.15 g, 2.0 mmol) were dissolved in aqueous methanol solution

(10 mL, 1:1 v/v). The mixture was stirred for 1 h to give a yellow solution, which was added to a stirred methanol of  $\text{CuSO}_4 \cdot 5\text{H}_2\text{O}$  (0.5 g, 2 mmol, 10 mL). The mixture was stirred for another 10 min at room temperature and then filtered. The filtrate was kept in air for 9d, forming blue block-shaped crystals of **1**. The crystals were isolated, washed three times with MeOH and dried in a vacuum desiccator containing anhydrous  $\text{CaCl}_2$ . Yield: 43%. *Anal.* Calc. for  $[(\text{CuL}_1)_2 \cdot 1/3(\text{CH}_3\text{OH})]_n$ : C, 44.59; H, 3.34; N, 5.57. Found: C, 44.60; H, 3.47; N, 5.30%. IR (KBr,  $\text{cm}^{-1}$ ): 3094, 3030, 1649, 1636, 1614, 1601, 1571, 1534, 1447, 1372, 1339, 1301, 1195, 1128, 1094, 796, 769. UV–Vis (DMSO– $\text{H}_2\text{O}$ ,  $\lambda/\text{nm}$ ): 251, 264, 368.

#### 2.2.2. Synthesis of $[\text{CuL}^2(\text{Py})(\text{H}_2\text{O})](\text{ClO}_4) \cdot \text{H}_2\text{O}$ (**2**)

Salicylaldehyde (0.24 g, 2.0 mmol) and *N*-(2-aminoethyl)morpholine (0.26 g, 2.0 mmol) were dissolved in pyridine and methanol mixture (10 mL, 10:1 v/v). The mixture was stirred for 30 min to give a yellow solution, which was added to a stirred methanol of  $\text{Cu}(\text{ClO}_4)_2 \cdot 7\text{H}_2\text{O}$  (0.78 g, 2.0 mmol, 10 mL). The mixture was stirred for another 10 min at room temperature and then filtered. The filtrate was kept in air for 7d, forming blue block-shaped crystals of **2**. The crystals were isolated, washed three times with MeOH and dried in a vacuum desiccator containing anhydrous  $\text{CaCl}_2$ . Yield: 51%. *Anal.* Calc. for  $[(\text{CuL}_2)(\text{Py})(\text{H}_2\text{O})](\text{ClO}_4) \cdot \text{H}_2\text{O}$ : C, 42.27; H, 5.12; N, 8.22. Found: C, 42.20; H, 5.37; N, 8.11%. IR (KBr,  $\text{cm}^{-1}$ ): 3513, 3339, 3232, 1643, 1608, 1600, 1540, 1471, 1448, 1343, 1314, 1100, 1090, 1070, 1051, 908, 751. UV–Vis (DMSO– $\text{H}_2\text{O}$ ,  $\lambda/\text{nm}$ ): 256, 268, 301, 370.

#### 2.2.3. Synthesis of $[\text{Cu}(\text{L}^3)_2] \cdot 2\text{H}_2\text{O}$ (**3**) and $[\text{Ni}(\text{L}^3)_2] \cdot 2\text{H}_2\text{O}$ (**4**)

Schiff-base ligand  $\text{HL}^3$  (0.48 g, 2.0 mmol) derived from condensation of salicylaldehyde and 4-(2-aminoethyl)phenylic acid was dissolved in methanol solution. The mixture was stirred for 30 min to give an orange solution, which was added to a stirred methanol of  $\text{CuCl}_2 \cdot 2\text{H}_2\text{O}$  (0.34 g, 2.0 mmol, 10 mL). The mixture was stirred for another 10 min at room temperature and then filtered. The filtrate was kept in air for 7d, forming deep-blue block-shaped crystals of **3**. The crystals were isolated, washed three times with MeOH and dried in a vacuum desiccator containing anhydrous  $\text{CaCl}_2$ . Yield: 29%. *Anal.* Calc. for  $(\text{CuL}^3)_2 \cdot 2\text{H}_2\text{O}$ : C, 62.11; H, 5.56; N, 4.83. Found: C, 62.00; H, 5.63; N, 4.81%. IR (KBr,  $\text{cm}^{-1}$ ): 3235(br), 1620, 1598, 1547, 1514, 1473, 1449, 1439, 1385, 1296, 1271, 1229, 1204, 1152, 1127, 1102, 827, 764. UV–Vis (DMSO– $\text{H}_2\text{O}$ ,  $\lambda/\text{nm}$ ): 251, 269, 307, 366.

Schiff-base ligand  $\text{HL}^3$  (0.48 g, 2.0 mmol) was dissolved in methanol solution. The mixture was stirred for 30 min to give an orange solution, which was added to a stirred methanol of  $\text{NiCl}_2 \cdot 6\text{H}_2\text{O}$  (0.48 g, 2.0 mmol, 10 mL). The mixture was stirred for another 10 min at room temperature and then filtered. The filtrate was kept in air for 7d, forming yellow block-shaped crystals of **4**. The crystals

were isolated, washed three times with MeOH and dried in a vacuum desiccator containing anhydrous CaCl<sub>2</sub>. Yield: 71%. *Anal. Calc.* for (NiL<sup>3</sup>)<sub>2</sub>·2H<sub>2</sub>O: C, 62.63; H, 5.61; N, 4.87. Found: C, 62.61; H, 5.70; N, 4.77%. IR (KBr, cm<sup>-1</sup>): 3202(br), 1614, 1597, 1550, 1514, 1473, 1442, 1350, 1295, 1270, 1230, 1152, 1127, 1103, 828, 764. UV–Vis (DMSO–H<sub>2</sub>O, λ/nm): 252, 272, 317, 373.

#### 2.2.4. Synthesis of [Ni(L<sup>4</sup>)<sub>2</sub>] (5) and [Mn<sub>2</sub>(L<sup>4</sup>)<sub>2</sub>(N<sub>3</sub>)<sub>2</sub>]·2CH<sub>3</sub>OH (6)

Schiff-base ligand HL<sup>4</sup> (0.61 g, 2.0 mmol) derived from condensation of salicylaldehyde and 4-(2-aminoethyl)benz-sulfamide was dissolved in methanol solution. The mixture was stirred for 30 min to give a yellow solution, which was added to a stirred methanol of NiCl<sub>2</sub>·6H<sub>2</sub>O (0.48 g, 2.0 mmol, 10 mL). The mixture was stirred for another 10 min at room temperature and then filtered. The filtrate was kept in air for 7d, forming black block-shaped crystals of 5. The crystals were isolated, washed three times with MeOH and dried in a vacuum desiccator containing anhydrous CaCl<sub>2</sub>. Yield: 29%. *Anal. Calc.* for Ni(L<sup>4</sup>)<sub>2</sub>: C, 54.15; H, 4.54; N, 8.42. Found: C, 53.77; H, 4.85; N, 8.40%. IR (KBr, cm<sup>-1</sup>): 3357, 3265, 1613, 1599, 1541, 1470, 1448, 1401, 1335, 1300, 1216, 1152, 1127, 1091, 1031, 876, 758. UV–Vis (DMSO–H<sub>2</sub>O, λ/nm): 252, 265, 319, 373.

Schiff-base ligand HL<sup>4</sup> (0.48 g, 2.0 mmol), Mn(AC)<sub>2</sub>·4H<sub>2</sub>O (0.50 g, 2.0 mmol) and sodium azide (0.065 g, 1 mmol) was dissolved in 20 mL methanol solution. The mixture was stirred for 30 min to give a brown solution. The mixture was stirred for another 10 min at room temperature and then filtered. The filtrate was kept in air for 8d, forming black block-shaped crystals of 6. The crystals were isolated, washed three times with MeOH and dried in a vacuum desiccator containing anhydrous CaCl<sub>2</sub>. Yield: 44%. *Anal. Calc.* for [Mn<sub>2</sub>(L<sup>4</sup>)<sub>2</sub>(N<sub>3</sub>)<sub>2</sub>]·2CH<sub>3</sub>OH: C, 50.61; H, 4.65; N, 13.33. Found: C, 50.71; H, 4.60; N, 13.20%.

IR (KBr, cm<sup>-1</sup>): 3605, 3307, 3252, 2055, 1609, 1544, 1470, 1445, 1405, 1338, 1309, 1222, 1159, 1123, 1093, 1009, 820, 756. UV–Vis (DMSO–H<sub>2</sub>O, λ/nm): 257, 271, 298, 385.

### 2.3. Inhibitory enzyme bioactivities tests

#### 2.3.1. Measurement of inhibitory activity against jack bean urease

Jack bean urease was purchased from Sigma–Aldrich Co. (St. Louis, Mo, USA). The measurement of urease was carried out according to the literature reported by Tanaka [25]. Generally, the assay mixture, containing 25 μL of Jack bean urease (10 kU/L) and 25 μL of the tested complexes of various concentrations (dissolved in the solution of DMSO:H<sub>2</sub>O = 1:1 (v/v)), was preincubated for 1 h at 37 °C in a 96-well assay plate. After preincubation, 0.2 mL of 100 mM HEPES (*N*-[2-hydroxy-ethyl] piperazine-*N'*-[2-ethanesulfonic acid]) buffer [26] pH = 6.8 containing 500 mM urea and 0.002% phenol red were added and incubated at 37 °C. The reaction time was measured by micro plate reader (570 nm), which was required to produce enough ammonium carbonate to raise the pH of a HEPES buffer from 6.8 to 7.7, the end-point being determined by the color of phenol red indicator [27].

#### 2.3.2. Measurement of inhibitory activity against XO

Xanthine oxidase from cow's milk was purchased from Sigma–Aldrich Co. (St. Louis, Mo, USA). The XO activities with xanthine as the substrate were measured spectrophotometrically, based on the procedure reported by Kong et al. [28], with modification. The assay was performed in a final volume of 1 mL 20 mM HEPES buffer pH 7.8 in quartz cuvette. Generally, the assay mixture, 100 μL 25 mU/mL XO, 50 μL of the various concentrations tested

Table 1  
Crystal data for complexes 1–6

Compound	1	2	3	4	5	6
Empirical formula	C <sub>18.67</sub> H <sub>16.67</sub> N <sub>2</sub> O <sub>6.67</sub> Cu <sub>2</sub>	C <sub>18</sub> H <sub>26</sub> N <sub>3</sub> O <sub>8</sub> ClCu	C <sub>30</sub> H <sub>32</sub> N <sub>2</sub> O <sub>6</sub> Cu	C <sub>30</sub> H <sub>32</sub> N <sub>2</sub> O <sub>6</sub> Ni	C <sub>30</sub> H <sub>32</sub> N <sub>4</sub> O <sub>6</sub> S <sub>2</sub> Ni	C <sub>62</sub> H <sub>68</sub> N <sub>14</sub> O <sub>14</sub> S <sub>4</sub> Mn <sub>2</sub>
Molecular weight	502.75	511.41	580.13	575.27	667.43	1469.41
Crystal system	monoclinic	monoclinic	orthorhombic	orthorhombic	triclinic	triclinic
Space group	<i>R</i> -3	<i>P</i> 2(1)/ <i>n</i>	<i>P</i> <i>bcn</i>	<i>P</i> <i>bcn</i>	<i>P</i> $\bar{1}$	<i>P</i> $\bar{1}$
<i>a</i> (Å)	26.991(7)	10.123(2)	15.482(2)	15.370(2)	10.011(2)	11.912(2)
<i>b</i> (Å)	26.991(7)	12.683(3)	10.782(2)	10.914(2)	10.473(2)	12.301(2)
<i>c</i> (Å)	6.987(4)	18.024(4)	15.957(2)	15.659(2)	16.499(2)	13.781(2)
$\alpha$ (°)	90.00	90.00	90.00	90.00	106.98(2)	116.06(2)
$\beta$ (°)	90.00	103.24(3)	90.00	90.00	90.02(2)	111.03(2)
$\gamma$ (°)	120.00	90.00	90.00	90.00	117.46(2)	91.46(2)
<i>T</i> (K)	295(2)	293(2)	292(2)	293(2)	292(2)	293(2)
<i>V</i> (Å <sup>3</sup> )	4408.5(3)	2253(8)	2663.9(5)	2626.9(4)	1449.3(4)	1652.2(4)
<i>Z</i>	9	4	4	4	2	1
$\rho_{\text{calc}}$ (g cm <sup>-3</sup> )	1.704	1.508	1.402	1.409	1.529	1.477
<i>F</i> (000)	2286	1060	1172	1168	696	762
$\mu$ (Mo K $\alpha$ ) (mm <sup>-1</sup> )	2.213	1.137	0.863	0.782	0.866	0.584
Data/restraint/parameters	2245/13/133	4835/3/280	3039/0/179	2723/0/175	6277/0/393	7425/0/436
Goodness-of-fit on <i>F</i> <sup>2</sup>	1.121	0.983	0.943	1.061	1.003	0.990
Final <i>R</i> <sub>1</sub> , <i>wR</i> <sub>2</sub> [ <i>I</i> > 2 $\sigma$ ( <i>I</i> )]	0.031, 0.095	0.063, 0.163	0.049, 0.127	0.060, 0.183	0.054, 0.137	0.050, 0.122

Table 2  
Selected bond lengths (Å) and angles (°) in complexes **1–6**

Compound 1			
Cu1–N1	1.927(2)	N1–Cu1–O3	92.98(7)
Cu1–O1	1.937(2)	O1–Cu1–O3	174.68(7)
Cu1–O3	1.947(2)	N1–Cu1–O3 <sup>[a]</sup>	162.10(7)
Cu1–O3 <sup>[a]</sup>	1.993(2)	O1–Cu1–O3 <sup>[a]</sup>	101.84(7)
Cu1–O2 <sup>[b]</sup>	2.259(2)	O3–Cu1–O3 <sup>[a]</sup>	79.95(7)
Cu1–Cu1 <sup>[a]</sup>	3.020(5)	N1–Cu1–O2 <sup>[b]</sup>	102.83(8)
O2–Cu1 <sup>[c]</sup>	2.258(2)	O1–Cu1–O2 <sup>[b]</sup>	93.85(8)
O3–Cu1 <sup>[a]</sup>	1.993(2)	O3–Cu1–O2 <sup>[b]</sup>	91.03(7)
N1–Cu1–O1	83.85(7)	O3 <sup>[a]</sup> –Cu1–O2 <sup>[b]</sup>	93.79(7)
Compound 2			
Cu1–O1	1.974(4)	O1–Cu1–N2	176.44(2)
Cu1–N1	1.978(4)	N1–Cu1–N2	84.71(2)
Cu1–N3	2.055(5)	N3–Cu1–N2	94.77(2)
Cu1–N2	2.139(5)	O1–Cu1–O3W	91.55(2)
Cu1–O3W	2.495(5)	N1–Cu1–O3W	90.85(2)
O1–Cu1–N1	92.84(2)	N3–Cu1–O3W	101.58(2)
O1–Cu1–N3	87.07(2)	N2–Cu1–O3W	91.07(2)
N1–Cu1–N3	167.56(2)		
Compound 3			
Cu1–O1	1.903(2)	O1–Cu1–N1	89.96(9)
Cu1–O1 <sup>[a]</sup>	1.903(2)	O1 <sup>[a]</sup> –Cu1–N1	90.04(9)
Cu1–N1	1.995(2)	O1–Cu1–N1 <sup>[a]</sup>	90.04(9)
Cu1–N1 <sup>[a]</sup>	1.995(2)	O1 <sup>[a]</sup> –Cu1–N1 <sup>[a]</sup>	89.96(9)
O1–Cu1–O1 <sup>[a]</sup>	180.00(2)	N1–Cu1–N1 <sup>[a]</sup>	180.00(2)
Compound 4			
Ni1–O1 <sup>[a]</sup>	1.834(2)	O1 <sup>[a]</sup> –Ni1–N1 <sup>[a]</sup>	89.52(2)
Ni1–O1	1.834(2)	O1–Ni1–N1 <sup>[a]</sup>	90.48(2)
Ni1–N1 <sup>[a]</sup>	1.939(3)	O1 <sup>[a]</sup> –Ni1–N1	90.48(2)
Ni1–N1	1.939(3)	O1–Ni1–N1	89.52(2)
O1 <sup>[a]</sup> –Ni1–O1	180.00(1)	N1 <sup>[a]</sup> –Ni1–N1	180.00(1)
Compound 5			
Ni1–O1 <sup>[a]</sup>	1.842(2)	Ni2–O4	1.832(2)
Ni1–O1	1.842(2)	Ni2–O4 <sup>[b]</sup>	1.832(2)
Ni1–N1 <sup>[a]</sup>	1.927(3)	Ni2–N3 <sup>[b]</sup>	1.922(2)
Ni1–N1	1.927(3)	Ni2–N3	1.922(2)
O1 <sup>[a]</sup> –Ni1–O1	180.00(1)	O4 <sup>[b]</sup> –Ni2–O4	180.0(2)
O1 <sup>[a]</sup> –Ni1–N1 <sup>[a]</sup>	91.28(2)	O4–Ni2–N3 <sup>[b]</sup>	87.48(2)
O1 <sup>[a]</sup> –Ni1–N1	88.72(2)	O4 <sup>[b]</sup> –Ni2–N3 <sup>[b]</sup>	92.52(2)
O1–Ni1–N1 <sup>[a]</sup>	88.72(2)	O4–Ni2–N3	92.52(2)
O1–Ni1–N1	91.28(2)	O4 <sup>[b]</sup> –Ni2–N3	87.48(2)
N1–Ni1–N1 <sup>[a]</sup>	180.00(2)	N3 <sup>[b]</sup> –Ni2–N3	180.00(2)
Compound 6			
Mn1–O1	1.855(2)	N1–Mn1–N2	179.34(8)
Mn1–O2	1.898(2)	O1–Mn1–N5	96.43(9)
Mn1–N1	2.038(2)	O2–Mn1–N5	96.54(9)
Mn1–N2	2.051(2)	N1–Mn1–N5	92.73(9)
Mn1–N5	2.163(2)	N2–Mn1–N5	87.88(9)
Mn1–O2 <sup>[a]</sup>	2.519(2)	O1–Mn1–O2 <sup>[a]</sup>	91.44(7)
O1–Mn1–O2	166.58(8)	O2–Mn1–O2 <sup>[a]</sup>	75.30(7)
O1–Mn1–N1	90.07(8)	N1–Mn1–O2 <sup>[a]</sup>	93.28(7)
O2–Mn1–N1	92.74(7)	N2–Mn1–O2 <sup>[a]</sup>	86.16(6)
O1–Mn1–N2	89.61(7)	N5–Mn1–O2 <sup>[a]</sup>	170.08(7)
O2–Mn1–N2	87.44(7)		

Symmetry transformations used to generate equivalent atoms. Complex **1**: [a]  $1/3 - x, 2/3 - y, 2/3 - z$ ; [b]  $-1/3 - x + y, 1/3 - x, 1/3 + z$ ; [c]  $1/3 - y, 2/3 + x - y, z - 1/3$ ; **3**: [a]  $-x, 1 - y, -z$ ; **4**: [a]  $2 - x, 1 - y, 1 - z$ ; **5**: [a]  $1 - x, 1 - y, 2 - z$ ; [b]  $-x, 1 - y, -z$ ; **6**: [a]  $2 - x, 1 - y, 1 - z$ .

complexes (dissolved in the solution of DMSO:H<sub>2</sub>O = 1:1) and 700  $\mu$ L of 50 mM HEPES buffer were preincubated for 1 h at 37 °C. After preincubation, the reaction is started by

addition 200  $\mu$ L of 84.8  $\mu$ g/mL xanthine in 50 mM HEPES. The reaction is monitored for 6 min at 295 nm at 37 °C and the product is expressed as  $\mu$ mol uric acid per minute.

#### 2.4. Crystal structure determination

Diffraction intensities for the six complexes were collected at 292(2)–295(2) K using a Bruker SMART CCD area detector with Mo K $\alpha$  radiation ( $\lambda = 0.71073$  Å). The collected data were reduced using the SAINT program [29], and empirical absorption corrections were performed using the SADABS program [30]. The structures were solved by direct methods and refined against  $F^2$  by full-matrix least-squares methods using the SHELXTL version 5.1 [31]. All of the non-hydrogen atoms were refined anisotropically. All other hydrogen atoms were placed in geometrically ideal positions and constrained to ride on their parent atoms. The crystallographic data for six complexes are summarized in Table 1. Selected bond lengths and angles are given in Table 2.

### 3. Results and discussion

#### 3.1. General aspects

The complexes have been characterized from the elemental analytical and spectral data, respectively. The IR spectra of complexes **1–6** exhibit strong absorption at 1609–1649  $\text{cm}^{-1}$ , assignable to the  $\nu(\text{C}=\text{N})$  absorption [32]. For **1**, the 1614 and 1601  $\text{cm}^{-1}$  bands are assigned to the  $\nu_{\text{asym}}(\text{COO})$  and  $\nu_{\text{sym}}(\text{COO})$ , respectively. The fact that  $\Delta\nu$  [ $\Delta\nu = \nu_{\text{asym}}(\text{COO}) - \nu_{\text{sym}}(\text{COO})$ ] is largely less than 200  $\text{cm}^{-1}$  demonstrates that the carboxylate group is coordinated as a bidentate ligand [33]. For **2**, the strong absorption peak for vibration of  $\text{ClO}_4^-$  is observed at about 1090  $\text{cm}^{-1}$ . For **3** and **4**, the appearances of the broad strong absorption at about 3230  $\text{cm}^{-1}$  can be reasonably attributed to the presence of lattice water molecule and/or phenolic OH group. The IR spectra of **5** and **6** show strong bands at 1613 and 1609  $\text{cm}^{-1}$  related to the  $\nu(\text{C}=\text{N})$  of the Schiff-base moiety, respectively, which are less than the corresponding value reported for their Schiff-base ligand [24]. This indicates coordination of the imine nitrogen to Ni<sup>2+</sup> and Mn<sup>3+</sup>. The strong absorption at 1300–1338  $\text{cm}^{-1}$  is attributed to the stretching vibration of S=O groups. Peak at 2055  $\text{cm}^{-1}$  in the IR spectrum of **6** is due to asymmetric stretching of the azide group [5b]. The UV–Vis spectra for the complexes **1–6** were obtained in assay condition (DMSO:H<sub>2</sub>O, 1:1 v/v). All the complexes show a weak d–d band in more than 500 nm region. In addition, the complexes exhibit intense bands in the 366–385 nm regions, which are attributed to a charge transfer (CT) transition [8,34]. For complex **2–6**, an absorption band at about 310 nm may also be associated with charge transfer and/or  $n \rightarrow \pi^*$  transitions [35].

The intense higher-energy bands at around 260 nm can be attributed to intraligand  $\pi \rightarrow \pi^*$  transitions.

### 3.2. Synthesis

Although imine bonds are susceptible to hydrolysis, metal complexes of Schiff bases are usually resistant towards hydrolytic cleavage, and as a result Schiff-base ligand  $H_2L^1$  was obtained from the condensation of salicylaldehyde with glycine in aqueous methanol solution (1:1 v/v) (see Section 2). In order to get better single-crystal, complex **1** was prepared by the reaction of Schiff-base ligand  $H_2L^1$  and  $CuSO_4 \cdot 5H_2O$  in aqueous methanol solution (1:1 v/v) too. Schiff-base ligand  $HL^2$  was obtained from the condensation of salicylaldehyde with *N*-(2-aminoethyl)morpholine in anhydrous methanol solution. However, complex **2** was prepared by the reaction of Schiff-base ligand  $HL^2$  and  $Cu(ClO_4)_2 \cdot 7H_2O$  in pyridine and methanol mixture (10:1 v/v). As previously reported in the literature, Schiff-base ligands  $HL^3$  and  $HL^4$  were obtained from the condensations of salicylaldehyde with 4-(2-aminoethyl)phenylic acid and 4-(2-aminoethyl)benz-sulfamide, respectively. Complexes **3** and **4**, showing metal ion  $Cu^{2+}$  and  $Ni^{2+}$  exchange were prepared by the reactions of Schiff-base ligand  $HL^3$  and  $CuCl_2 \cdot 2H_2O$  and  $NiCl_2 \cdot 6H_2O$  in the same condition, respectively. Complex **6** were prepared by the reactions of Schiff-base ligand  $HL^4$ ,  $Mn(AC)_2 \cdot 4H_2O$  and  $NaN_3$  (molar ratio = 1:1:05).

### 3.3. Crystal structure description

#### 3.3.1. $[(CuL^1)_2 \cdot 1/3(CH_3OH)]_n$ (**1**)

The structure of complex **1** consists of a three-dimensional network motif which is constructed through the dinuclear moieties  $[Cu(L^1)]_2$  and the disordered lattice methanol molecules as shown Fig. 1. In **1**, the moieties  $[Cu(L^1)]_2$ , which lies on a center-of-inversion, were bridged through the double-bond carbonyl O atoms into a three-dimensional network motif whose cavities are occupied by the disordered lattice methanol. The dinuclear unit  $[Cu(L^1)]_2$  is formed by two Cu atoms labeled Cu1 and Cu1A [symmetry code:  $1/3 - x, 2/3 - y, 2/3 - z$ ], bridged by the two  $\mu_2$ -phenolato oxygen atom O3 and O3A of Schiff-base ligands ( $L^1$ ) (Scheme 1). Each copper atom is in a square pyramidal geometry and is five-coordinated by one nitrogen atom and four oxygen atoms from three independent *N*-salicylidene-glycinate ligands, respectively. The copper metal ion locates 0.025 Å above the basal plane, which is constituted via N1, O1, O3, O3A atoms, toward the apical site of the square pyramidal geometry which is taken up by the bridging carbonyl O atom of an adjacent dimer  $[Cu1-O2 \ 2.258(2) \text{ \AA}]$ . The bond lengths in the basal plane are Cu1-N1 1.927(2); Cu1-O1 1.937(2); Cu1-O3 1.947(2); Cu1-O3A 1.993(2) Å. The Cu...Cu distance of 3.02 Å falls in the relatively small range of 2.93–3.10 Å, showing the weak metal–metal inter-

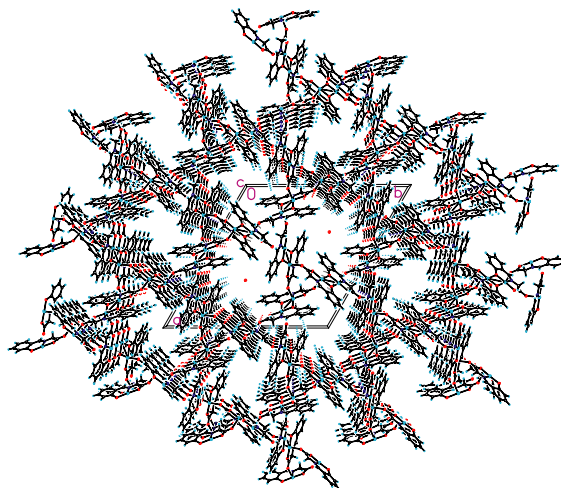
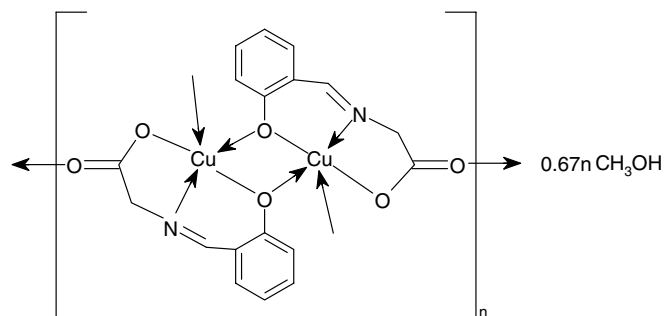


Fig. 1. Molecular packing view of  $[(CuL^1)_2 \cdot 1/3(CH_3OH)]_n$  (**1**) along the *c*-axis; the disordered methanol solvent are shown as the red dots. (For interpretation of the references to colour in this figure legend, the reader is referred to the web version of this article.)

actions [36]. The *N*-salicylidene-glycinate dianion  $N,O,O'$ -chelates to one Cu atom and the dianion also uses its hydroxy O atom to form a dative bond to the other Cu atom so that one N and three O atoms comprise a square.  $trans-[(C_9H_7NO_3)Cu]_2$  can be regarded as a quasi-planar 4-connected building unit. The assembly of the 4-connected nodes results in the generation of three- and six-membered windows to form a desired channel structure along  $[001]$  (Fig. 1), giving an overall Kagomé lattice topology. The largest channel is about  $13.5 \times 13.5 \text{ \AA}^2$  in inner size, comparable to the porous or grid-like coordination polymers reported so far [37]. The methanol solvate is formally a dinuclear compound (Scheme 1), lying on a three-fold rotation axis and located in the wider areas of the channel, exagonal cavities.

#### 3.3.2. $[CuL^2(Py)(H_2O)](ClO_4) \cdot H_2O$ (**2**)

Complex **2** consists of the mononuclear units  $[CuL^2(Py)(H_2O)]$ , the perchlorate counter ions and the lattice water molecules as shown in Fig. 2. In the mononuclear unit of complex **2**, copper metal ion is in a square-pyramidal coordination with the apical site occupied by water



Scheme 1. The structure of complex **1**.

molecule [Cu1–O3w, 2.495(5) Å]. The basal plane of the square pyramid is occupied by one oxygen atom from phenolate group [Cu1–O1, 1.974(4) Å] and three nitrogen atoms from the imine group [Cu1–N1, 1.978(4) Å], the morpholine group [Cu1–N2, 2.139(5) Å], and pyridine group [Cu1–N3, 2.055(5) Å], respectively. The copper metal ion is 0.0159 Å above the basal plane towards the apical oxygen atom O3w of water molecule.

### 3.3.3. $[Cu(L^3)_2] \cdot 2H_2O$ (3) and $[Ni(L^3)_2] \cdot 2H_2O$ (4)

Recently, we have reported a Schiff base (HL<sup>3</sup>) derived from the condensation of salicylaldehyde with 4-(2-aminoethyl)phenylic acid, which has been structurally characterized [23]. Herein we report two metal complex 3 and 4 which were prepared from reactions of Cu<sup>2+</sup> and Ni<sup>2+</sup> with the ligand HL<sup>3</sup>, respectively. The molecular structures of 3 and 4 were ascertained by X-ray crystallography and were found to be structurally very similar. Perspective drawings of 3 and 4 are shown in Figs. 3 and 4, respectively, and selected bond lengths and bond angles are given in Table 2.

Both of them are the mononuclear complex of formula  $Cu(L^3)_2 \cdot 2H_2O$  and  $Ni(L^3)_2 \cdot 2H_2O$ , respectively. Complex 3 affords a square planar *trans*-[CuN<sub>2</sub>O<sub>2</sub>] coordination geometry, whose central Cu<sup>2+</sup> lies on the center of symmetry. The ligand L<sup>3</sup> acts as a bidentate ligand and coordinates to Cu<sup>2+</sup> through the phenolate O atom [Cu1–O1, 1.903(2) Å] and the N-donor [Cu1–N1, 1.995(2) Å] from the imine group. In the crystal structure of complex 4, Ni<sup>2+</sup> lies in the position as Cu<sup>2+</sup> of complex 3 does and is four-coordinate via the phenolate O atom and N-donor of the Schiff-base moiety. The bond distances of Ni1–O1 and Ni1–N1 are 1.834(2) and 1.939(3) Å, respectively, which are comparable with the corresponding values reported for nickel(II) species having the same coordinating atoms [38].

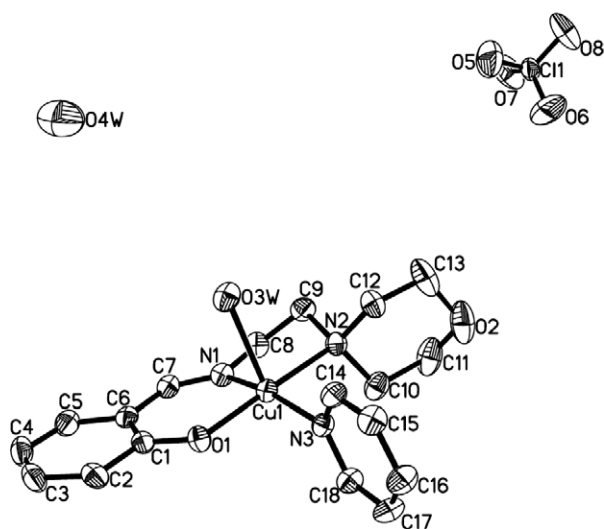


Fig. 2. ORTEP drawing of the molecular structure of  $[CuL^2(Py)(H_2O)](ClO_4) \cdot H_2O$  (2). Thermal ellipsoids are drawn at the 30% probability level and hydrogen atoms are omitted for clarity.

### 3.3.4. $[Ni(L^4)_2]$ (5) and $[Mn_2(L^4)_2(N_3)_2] \cdot 2CH_3OH$ (6)

The structure of the Schiff-base compound (HL<sup>4</sup>), derived from the condensation of salicylaldehyde with 4-(2-aminoethyl)benzulfamide, was reported previously [24]. Herein we report two metal complexes 5 and 6 which were prepared from reactions of Ni<sup>2+</sup> and Mn<sup>2+</sup> with the ligand HL<sup>4</sup>, respectively. The molecular structures of 5 and 6 were ascertained by X-ray crystallography. Perspective drawings of 5 and 6 are shown in Figs. 5 and 6, respectively, and selected bond lengths and bond angles are given in Table 2. The former is a mononuclear complex of formula  $Ni(L^4)_2$ , while the latter is a dinuclear complex of formula  $Mn_2(L^4)_2(N_3)_2 \cdot 2CH_3OH$ . In the crystal structure of complex 5, there are two independent half-molecules per asymmetric unit. Each nickel metal ion lies on inversion centers and is four-coordinate by two deprotonated Schiff-base ligands (L<sup>4</sup>) through the phenolate O atoms [Ni1–O1, 1.842(2) Å; Ni2–O4, 1.832(2) Å] and the

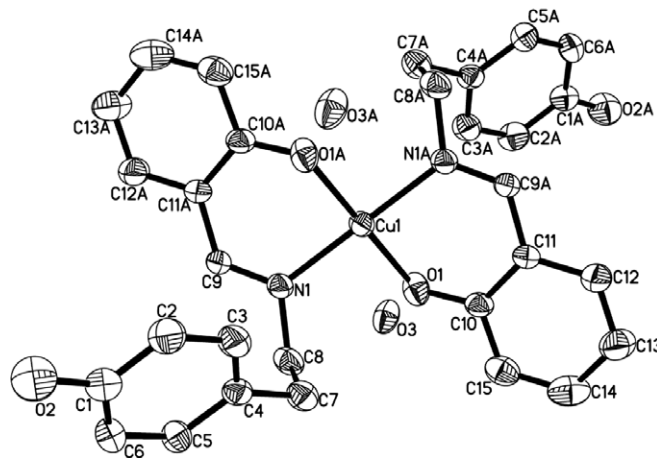


Fig. 3. ORTEP drawing of the molecular structure of  $[Cu(L^3)_2] \cdot 2H_2O$  (3). Thermal ellipsoids are drawn at the 30% probability level and hydrogen atoms are omitted for clarity.

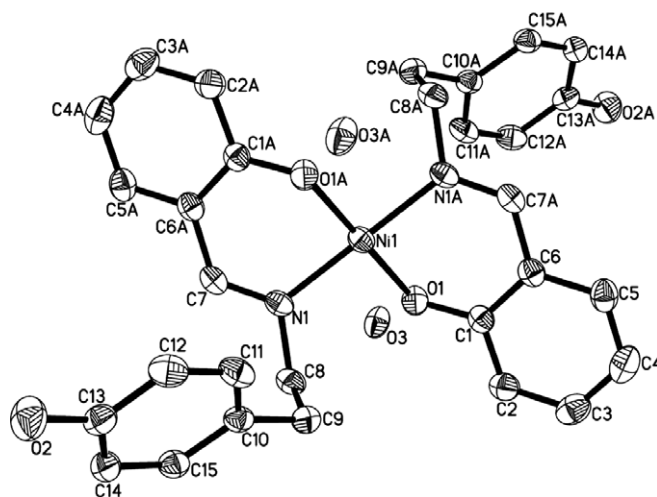


Fig. 4. ORTEP drawing of the molecular structure of  $[Ni(L^3)_2] \cdot 2H_2O$  (4). Thermal ellipsoids are drawn at the 30% probability level and hydrogen atoms are omitted for clarity.

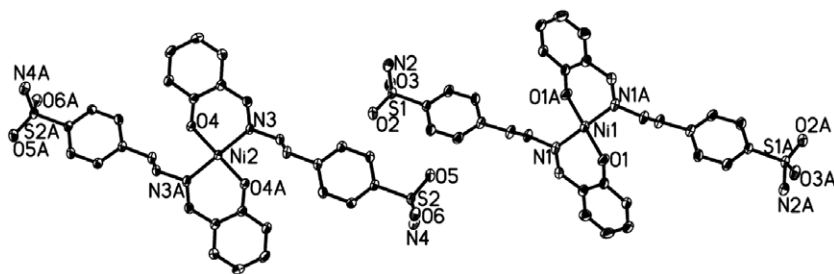


Fig. 5. ORTEP drawing of the molecular structure of  $[\text{Ni}(\text{L}^4)_2]$  (**5**). Thermal ellipsoids are drawn at the 30% probability level and C atoms not labeled and hydrogen atoms omitted for clarity.

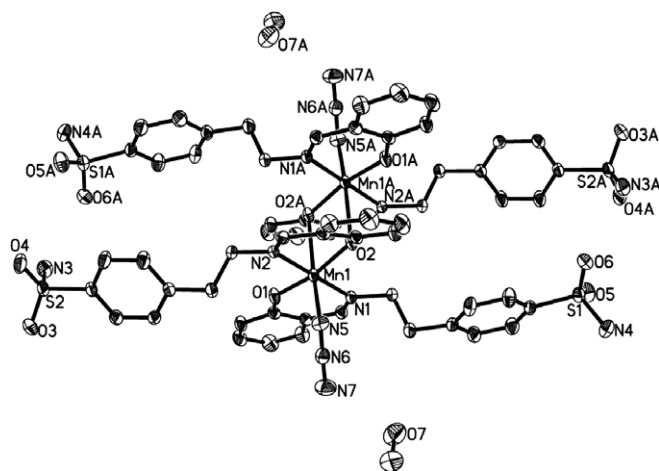


Fig. 6. ORTEP drawing of the molecular structure of  $[\text{Mn}_2(\text{L}^4)(\text{N}_3)_2] \cdot 2\text{CH}_3\text{OH}$  (**6**). Thermal ellipsoids are drawn at the 30% probability level and C atoms not labeled and hydrogen atoms omitted for clarity.

N-donors [Ni1–N1, 1.927(3) Å; Ni2–N3, 1.922(3) Å] from the imine groups to form a square-planar geometry surrounding  $\text{Ni}^{2+}$ . Complex **6** consists of a centrosymmetric dimer with manganese centers assuming a distorted octahedral coordination geometry and two methanol anions. The dinuclear unit is formed by two Mn atoms labeled Mn1 and Mn1A [symmetry code:  $2 - x, 1 - y, 1 - z$ ], bridged by the phenolic oxygen atoms O2 and O2A of the deprotonated Schiff-base ligands ( $\text{L}^4$ ), to construct an interesting square plane consisting of Mn1, O2, Mn1A, O2A. The Mn...Mn distance is 3.517(2) Å. At each manganese center, the equatorial plane of octahedral geometry is occupied by two phenolate O atoms [Mn1–O1, 1.855(2) Å; Mn1–O2, 1.897(2) Å] and two imine nitrogen atoms [Mn1–N1, 2.038(2) Å; Mn1–N2, 2.051(2) Å] from two deprotonated ligands ( $\text{L}^4$ ). The apical sites of the manganese centers have anti configuration and are occupied by the bridging oxygen atom [Mn1–O2A, 2.519(2) Å] from phenolate group of another deprotonated ligand ( $\text{L}^4$ ) and the nitrogen atom [Mn1–N5, 2.163(2) Å] from azide group.

### 3.4. Inhibitory bioactivities against jack bean urease and XO

#### 3.4.1. Inhibitory activity against jack bean urease

The ability of the complexes **1–6** in inhibiting urease has been studied by the  $\text{IC}_{50}$  values of the complexes (25  $\mu\text{L}$ ,

100  $\mu\text{g}$ ) tested against *jack bean* urease (25  $\mu\text{L}$ , 10 kU/L) using urea (500 mM) in HEPES buffer (0.2 mL, 100 mM; pH = 6.8). On reaction with *Jack bean* urease in the presence of phenol red, complexes **1–6** show inhibitory enzyme activity (Fig. 7). Under the same condition the Schiff-base ligands  $\text{L}^{1-4}$  as enzyme inhibitors have no ability to inhibit urease (see Table 3). This indicates the Schiff-base ligand have less influence on the activity of *jack bean* urease. Metal ions as enzyme inhibitors exhibit different ability to inhibit urease. Inhibitory efficiency of metal ions toward urease follows the order:  $\text{Cu}^{2+} > \text{Ni}^{2+} > \text{Mn}^{2+}$ , which has been reported in the literature [39]. To my surprise, the abilities of these complexes to inhibit urease follow the order: **2** > **3** > **1** > **4** > **6** > **5**.

For these transition metal complexes used as urease inhibitors, copper(II) complexes exhibit stronger ability to inhibit urease due to the strong Lewis acid properties of copper metal ions. Among these copper complexes complex **2** exhibited strongest ability to inhibit urease probably because of copper metal ion being in the square-pyramidal coordination and simple molecular structure. In contrast, complex **1** exhibited weaker ability

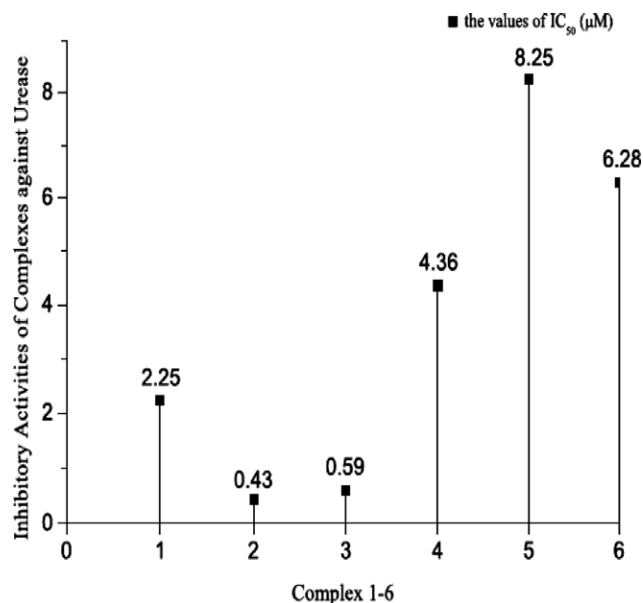


Fig. 7. The inhibitory activities of complexes **1–6** against urease.

Table 3  
The average IC<sub>50</sub> values (in μM) of the tested compounds against urease and XO

Tested materials	Inhibition of urease activity	Inhibition of XO activity
H <sub>2</sub> L <sup>1</sup> (C <sub>9</sub> H <sub>9</sub> NO <sub>3</sub> )	>100	>100
HL <sup>2</sup> (C <sub>13</sub> H <sub>18</sub> N <sub>2</sub> O <sub>2</sub> )	>100	>100
HL <sup>3</sup> (C <sub>15</sub> H <sub>15</sub> NO <sub>2</sub> )	>100	>100
HL <sup>4</sup> (C <sub>15</sub> H <sub>16</sub> N <sub>2</sub> O <sub>3</sub> S)	>100	>100
Cu <sup>2+</sup>	0.37	1.24
Ni <sup>2+</sup>	2.87	>100
Mn <sup>2+</sup>	>100	>100
Positive controls	42.12 (acetohydroxamic acid)	10.37 (allopurinol)

to inhibit urease probably resulting from its molecular polymerization. The ability of complex **3** to inhibit the urease exhibits stronger than that of complex **4** although their crystal structures are very similar. This also shows that inhibitory efficiency of the complex toward urease: copper complex > nickel complex. However, complex **4** exhibits stronger ability to inhibit urease than complex **5** due to two different Schiff-base ligands (L<sup>3</sup> and L<sup>4</sup>), respectively. The former containing soluble phenolic hydroxy is in favor of inhibitory urease. Complex **5** has weaker inhibitory activity against urease than complex **6** in despite of containing the same Schiff-base ligand (L<sup>4</sup>). This shows that inhibitory efficiency of the complex toward urease may be influenced not only by the transition metal ion but also by ligands. To my surprise, complex **6** exhibit strong ability to inhibit the urease although manganese metal ion has no inhibitory activity of urease probably due to the reaction of Schiff-base ligand and Mn<sup>3+</sup>. Besides azide ligand probably strengthens inhibitory activity of **6**.

#### 3.4.2. Inhibitory activity against XO

The ability of the complexes **1–6** in inhibiting xanthine oxidase has been studied by the IC<sub>50</sub> values of the complexes (50 μL, 200 μg) tested against XO (100 μL, 25 mU/mL) using xanthine (200 μL, 84.8 μg/mL) in HEPES buffer (0.7 mL, 50 mM; pH = 7.8). On reaction with XO in the presence of uric acid, complexes **1–6** show inhibitory XO activity (Fig. 8). Under the same condition the Schiff-base ligands L<sup>1–4</sup> as XO inhibitors have no ability to inhibit XO (see Table 3). This indicates the Schiff-base ligands as XO inhibitors have no influence on the activity of XO. Only copper metal ion exhibits ability to inhibit XO among metal ions. To my surprise, the abilities of complexes obtained from reactions of Schiff-base ligands and these metal ions to inhibit XO follow the order: **2** > **3** > **1** > **4** ≈ **5** ≈ **6**. The ability of three copper complexes to inhibit XO is comparable to that of allopurinol, a well-known inhibitor of XO. The ability of complex **2** to inhibit XO exhibits the strongest among three copper complexes probably due to being in the square-pyramidal coordination and simple molecular structure, which is better to let inhibitor interact with active site of XO or

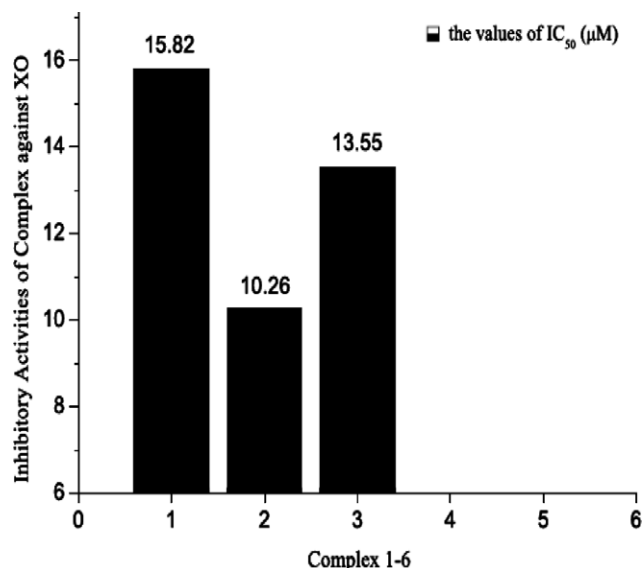


Fig. 8. The inhibitory activities of complexes **1–6** against XO (the IC<sub>50</sub> value that is more than 100 μM were not shown).

substrate of XO. As the inhibitor of XO, complex **1** shows weaker inhibitory activity probably owing to the molecular polymerization. Both nickel and manganese complexes **4–6** exhibit no ability to inhibit XO probably due to their metal character.

#### 4. Conclusion

The present report describes the syntheses, X-ray crystal structures and inhibitory enzyme activity of transition metal complexes (M = Cu, Ni, Mn) having salicylaldehyde Schiff-base ligands. The syntheses of these compounds are intriguing and their properties are strongly dependent on the kind of metal ions and organic ligands. Copper complexes **1–3** exhibit strong ability to inhibit activity of urease and xanthine oxidase. However, nickel and manganese complexes only exhibit ability to inhibit activity of urease, which may be potential selective enzyme inhibitors. Most of these complexes exhibit ideal ability to inhibit urease and XO. It's very interesting to study that as enzyme inhibitors Schiff-base complexes exhibit potential abilities to inhibit activities of urease and XO in order to discover novel urease and XO inhibitors. We have demonstrated for the first time that Schiff-base complexes show urease and XO inhibitory activities. The mechanisms of the inhibitory activity require to be further investigated.

#### Acknowledgement

This work was co-financed by grant (Project 30672516) from National Natural Science Foundation of China and by grant (Key Project 03085) from the State Education Ministry of China.

## References

- [1] M.R. Maurya, A. Kumar, A.R. Bhat, A. Azam, C. Bader, D. Rehder, *Inorg. Chem.* 45 (2006) 1260.
- [2] (a) S. Koner, S. Saha, T. Mallah, K.I. Okamoto, *Inorg. Chem.* 43 (2004) 840;  
(b) A.K. Sah, T. Tanase, M. Mikuriya, *Inorg. Chem.* 45 (2006) 2083.
- [3] Q.-F. Han, F.-F. Jian, L.-D. Lu, X.-J. Yang, X.-J. Wang, *Chem. Crystallog.* 31 (2001) 247.
- [4] A. Erxleben, D. Schumacher, *Eur. J. Inorg. Chem.* (2001) 3039.
- [5] (a) M.R. Bermejo, A.M. Gonzalez-Noya, V. Abad, M.I. Fernandez, M. Maneiro, R. Pedrido, M. Vazquez, *Eur. J. Inorg. Chem.* (2004) 3696;  
(b) Y.-B. Jiang, H.-Z. Kou, R.-J. Wang, A.-L. Cui, *Eur. J. Inorg. Chem.* (2004) 4608.
- [6] W. Wernsdorfer, R. Sessoli, *Science* 284 (1999) 133.
- [7] D. Imbert, S. Comby, A.-S. Chauvin, J.-C. Bünzli, *Chem. Commun.* (2005) 1432.
- [8] V.W.W. Yam, K.K.W. Lo, *Coord. Chem. Rev.* 184 (1999) 157.
- [9] A. Mukherjee, S. Dhar, M. Nethaji, A.R. Chakravarty, *J. Chem. Soc., Dalton Trans.* (2005) 349.
- [10] R. Häner, J. Hall, *Antisense Nucleic Acid Drug Dev.* 7 (1997) 423.
- [11] (a) J.B. Sumner, *J. Biol. Chem.* 69 (1926) 435;  
(b) N.E. Dixon, C. Gazzola, R.L. Blakeley, B. Zerner, *J. Am. Chem. Soc.* 97 (1975) 4131.
- [12] P.A. Karplus, M.A. Pearson, R.P. Hausinger, *Acc. Chem. Res.* 30 (1997) 330.
- [13] H.L.T. Mobley, M.D. Island, R.P. Hausinger, *Microbiol. Rev.* 59 (1995) 451.
- [14] Q. Zheng, O. Van Cleemput, P. Demeyer, L. Baert, *Biol. Fertil. Soils* 11 (1991) 41.
- [15] S. Benini, W.R. Rypniewski, K.S. Wilson, S. Mangani, S. Ciurli, *J. Am. Chem. Soc.* 126 (2004) 3714.
- [16] M.J. Todd, R.P. Hausinger, *Biochemistry* 39 (2000) 5389.
- [17] (a) W.H.R. Shaw, D.N. Raval, *J. Am. Chem. Soc.* 83 (1961) 3184;  
(b) B. Krajewska, *J. Chem. Technol. Biotechnol.* 52 (1991) 157;  
(c) C. Preininger, O.S. Wolfbeis, *Biosens. Bioelectron.* 11 (1996) 981.
- [18] T. Tanaka, M. Kawase, S. Tani, *Bioorgan. Med. Chem.* 12 (2004) 501.
- [19] (a) D.J. Hearse, A.S. Manning, J. Downey, D.M. Yellon, *Acta Physiol. Scand. Suppl.* 548 (1986) 65;  
(b) P.-H. Chan, J.W. Schimidley, R.A. Fishman, S.M. Longar, *Neurology* 34 (1984) 315.
- [20] H.S.D. Naeff, M.C.R. Franssen, H.C. van der Plas, *Recl. Trav. Pays-Bas* 110 (1991) 139.
- [21] R.K. Robins, G.R. Revankar, D.E. Ö'Brien, R.H. Springer, T. Novinson, A. Albert, K. Senga, J.P. Miller, D.G. Streeter, *J. Heterocycl. Chem.* 22 (1985) 601.
- [22] Z.-L. You, D.-S. Shi, H.-L. Zhu, *Inorg. Chem. Comm.* 9 (2006) 642.
- [23] Y.-G. Li, H.-L. Zhu, W.-Q. Huang, L. Ai, *Acta Crystallogr. Sect. E* 62 (2006) 689.
- [24] R.R. Coombs, M.K. Ringer, J.M. Blacquiere, J.C. Smith, J.S. Neilsen, Y.-S. Uh, J.B. Gilbert, L.J. Leger, H.-W. Zhang, A.M. Irving, S.L. Wheaton, C.M. Vogels, S.A. Westcott, A. Decken, F.J. Baerlocher, *Transit. Met. Chem.* 30 (2005) 411.
- [25] T. Tanaka, M. Kawase, S. Tani, *Life Sci.* 73 (2003) 2985.
- [26] W. Zaborska, B. Krajewska, Z. Olech, *J. Enzyme Inhib. Med. Chem.* 19 (2004) 65.
- [27] D.D. Van Slyke, R.M. Archibald, *J. Bio. Chem.* 154 (1994) 623.
- [28] L.-D. Kong, Y. Zhang, X. Pan, R.-X. Tan, C.H.K. Cheng, *Cell. Mol. Life Sci.* 57 (2000) 500.
- [29] Bruker, SMART (Version 5.628) and SAINT (Version 6.02), Bruker AXS Inc., Madison, Wisconsin, USA, 1998.
- [30] G.M. Sheldrick, SADABS. Program for Empirical Absorption Correction of Area Detector, University of Göttingen, Germany, 1996.
- [31] G.M. Sheldrick, SHELXTL V5.1 Software Reference Manual, Bruker AXS Inc., Madison, Wisconsin, USA.
- [32] (a) R. Klement, F. Stock, H. Elias, H. Paulus, P. Pelikán, M. Valko, M. Mazúr, *Polyhedron* 18 (1999) 3617;  
(b) T. Akitsu, Y. Einaga, *Polyhedron* 24 (2005) 1869;  
(c) M. Kettunen, A.S. Abu-Surrah, H.M. Abdel-Halim, T. Repo, M. Leskelä, M. Laine, I. Mutikainen, M. Ahlgren, *Polyhedron* 23 (2004) 1649.
- [33] (a) Á. García-Raso, J.J. Fiol, F. Bádenas, E. Lago, E. Molins, *Polyhedron* 20 (2001) 2877;  
(b) Ch.-J. Hu, W.-W. Zhang, Y. Xu, H.-Zh. Zhu, X.-M. Ren, Ch.-Sh. Lu, Q.-J. Meng, H.-Q. Wang, *Transit. Met. Chem.* 26 (2001) 700.
- [34] (a) J.B. Vincent, K. Foltling, J.C. Huffman, G. Christou, *Inorg. Chem.* 25 (1986) 996;  
(b) S.T. Lutta, S.M. Kagwanja, *Transit. Met. Chem.* 25 (2000) 415;  
(c) A. Panja, N. Shaikh, S. Gupta, R.J. Butcher, P. Banerjee, *Eur. J. Inorg. Chem.* (2003) 1540.
- [35] U. Mukhopadhyay, L.R. Falvello, D. Ray, *Eur. J. Inorg. Chem.* (2001) 2823.
- [36] (a) K. Itoh, H. Hayashi, H. Furutachi, T. Matsumoto, S. Nagatomo, T. Toshi, S. Ter-ada, S. Fujinami, M. Suzuki, T. Kitagawa, *J. Am. Chem. Soc.* 127 (2005) 5212;  
(b) N.N. Murthy, M. Mahroof-Tahir, K.D. Karlin, *Inorg. Chem.* 40 (2001) 628;  
(c) K.D. Karlin, P. Ghosh, R.W. Cruse, A. Farooq, Y. Gultneh, R.R. Jacobson, N.J. Blackburn, R.W. Strange, J. Zubieta, *J. Am. Chem. Soc.* 110 (1988) 6769;  
(d) M. Mahroof-Tahir, N.N. Murthy, K.D. Karlin, N.J. Blackburn, S.N. Shaikh, J. Zubieta, *Inorg. Chem.* 31 (1992) 3001.
- [37] (a) J. Zhang, M.M. Matsushita, X.X. Kong, J. Abe, T. Iyoda, *J. Am. Chem. Soc.* 123 (2001) 12105;  
(b) S.-i. Noro, S. Kitagawa, M. Kondo, K. Seki, *Angew. Chem., Int. Ed.* 39 (2000) 2082;  
(c) H.-L. Li, M. Eddaoudi, M. ÖKeeffe, O.M. Yaghi, *Nature* 402 (1999) 276;  
(d) K. Biradha, Y. Hongo, M. Fujita, *Angew. Chem., Int. Ed.* 39 (2000) 3843;  
(e) G.B. Gardner, D. Venkataraman, J.S. Moore, S. Lee, *Nature* 374 (1995) 792.
- [38] T. Akitsu, Y. Einaga, *Polyhedron* 24 (2005) 1869.
- [39] (a) W.H.R. Shaw, D.N. Raval, *J. Am. Chem. Soc.* 83 (1961) 3184;  
(b) B. Krajewska, *J. Chem. Technol. Biotechnol.* 52 (1991) 157.